CHALMERS
UNIVERSITY OF TECHNOLOGY

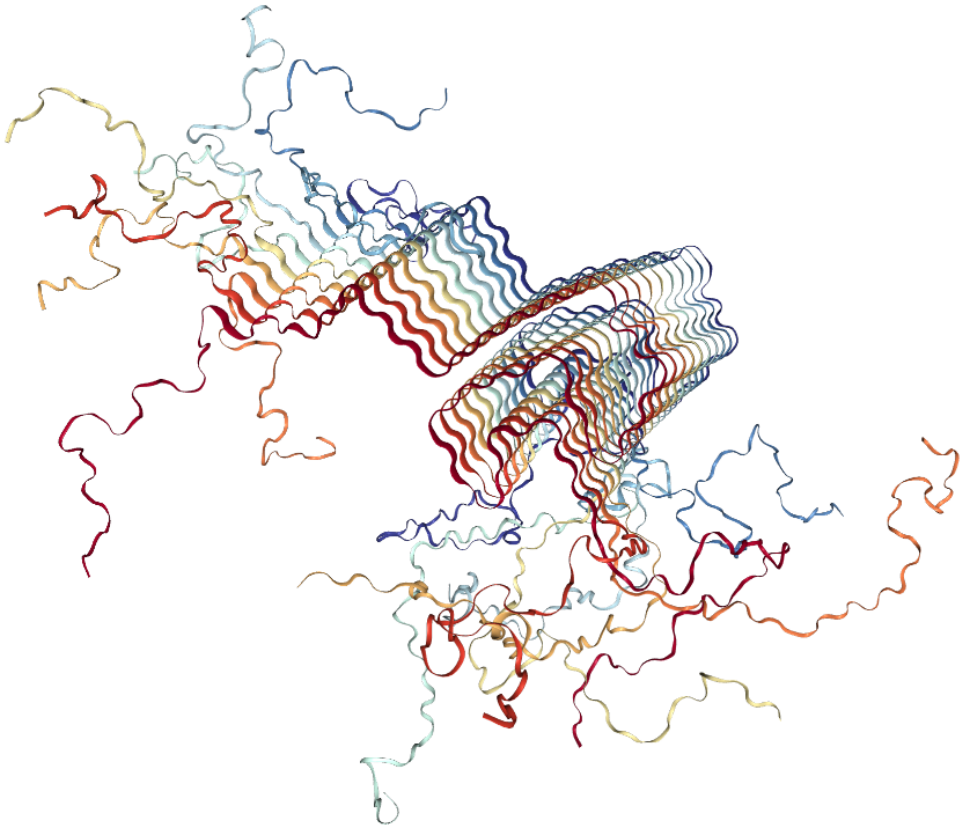

Effects of metal ions on aggregation of Parkinson's disease protein, α-synuclein

Master's thesis in Biotechnology

EMMA LORENTZON

Department of Biology and Biological Engineering
CHALMERS UNIVERSITY OF TECHNOLOGY
Gothenburg, Sweden 2019

Master's thesis 2019:48127

Effects of metal ions on aggregation of Parkinson's disease protein, α-synuclein.

Cu(II), Zn(II), Fe(III) and Mn(II)-ion effects on the aggregation kinetics of wild type, N-terminal acetylated, 97 a.a. truncated, and A53T mutated variants of α-synuclein.

EMMA LORENTZON

CHALMERS
UNIVERSITY OF TECHNOLOGY

Department of Biology and Biological Engineering
Division of Chemical Biology
Pernilla Wittung-Stafshede's research group
Chalmers University of Technology
Gothenburg, Sweden 2019

Effects of metal ions on aggregation of Parkinson's disease protein, α-synuclein.
Cu(II), Zn(II), Fe(III) and Mn(II)-ion effects on the aggregation kinetics of wild type, N-terminal acetylated, 97 a.a. truncated, and A53T mutated variants of α-synuclein.
EMMA LORENTZON

Supervisor: Istvan Horvath, Chemical biology
Examiner: Pernilla Wittung-Stafshede, Chemical biology

Master's Thesis 2019:48127
Department of Biology and Biological Engineering
Division of Chemical Biology
Chalmers University of Technology
SE-412 96 Gothenburg
Telephone +46 31 772 1000

Cover: α-synuclein amyloid fibril (Tuttle et al., 2016).

Typeset in LaTeX
Gothenburg, Sweden 2019

Effects of metal ions on aggregation of Parkinson's disease protein, α-synuclein.

EMMA LORENTZON
Department of Biology and Biological Engineering
Chalmers University of Technology

Abstract

Parkinson's disease (PD) is one of the most common neurodegenerative diseases worldwide. The pathology of the disease is characterized by the loss of dopaminergic neurons in the motor center of the brain, substantia nigra, coupled with amyloid aggregates of α-synuclein (α-syn) in the cytoplasm known as Lewy bodies. The brain has tight control of metal ions homeostasis but is known to accumulate metal over time. Researches have previously noted the increase of metal ions in PD patients brains, and a high concentration of iron has been found in Lewy bodies. Evidence suggests that disrupted metal homeostasis may play an important role in the development of neurodegenerative diseases, by causing oxidative stress and abnormal interactions with proteins. α-syn has been shown to be a metal binding protein, and its interactions with metals may play a role in the aggregation kinetics. α-syn can exist in many forms; C-terminally truncated, with disease-promoting mutations (e.g. A53T), and it was recently shown to be N-terminal acetylated *in vivo*. These versions are important to study to gain a better understanding of metal-interactions and their role in aggregation. In this thesis, I studied α-syn aggregation in the presence of the biochemically active metals copper (Cu(II)), iron (Fe(III)), manganese (Mn(II)) and zinc (Zn(II)). This was done using ThT-fluorescence aggregation assays to compare aggregation kinetics, circular dichroism (CD) to study the tertiary structure and metal binding, and imaging of the fibrils with atomic force microscopy (AFM) and transmission electron microscopy (TEM).

The results in this thesis show the importance of Fe(III) in the aggregation kinetics for α-syn wild-type (WT), A53T and acetylated α-syn. Cu(II) had less impact on the aggregation of acetylated protein; in accord with the N-terminus being important in Cu-binding. This also suggests a less important role of Cu(II) in α-syn aggregation *in vivo*. Truncated α-syn aggregation kinetics was not affected by the metal ions, suggesting that metal binding occurs in the missing C-terminal, or its aggregation was too fast to be affected by metals binding. Mn(II) and Zn(II) did not affect any α-syn versions' aggregation; indicating weak or no binding of the metal ions, and thus no direct effect on aggregation.

Keywords: alpha synuclein, aggregation kinetics, Parkinson's disease, metal interaction, copper, iron, zinc, manganese

Acknowledgements

I would like to express my gratitude to Professor Pernilla Wittung-Stafshede, examiner of this Master's thesis, for giving me with the opportunity to be part of her team, and work on this project for these last six months. I would also like to thank my supervisor Istvan Horvath for all the generous time and knowledge he has given me during this project. The valuable feedback and enthusiastic encouragement throughout the work has been greatly appreciated from them both.
A big thank you to the Chemical biology division for enduring all of my questions, welcoming me, and helping me as much as you did. Special thank you to Ranjeet Kumar for the protein used in this project. A final thank you to friends and family for continued support through these five years of studies at Chalmers.

Emma Lorentzon, Gothenburg, June 2019

Contents

List of Figures **xi**

1 Introduction **1**
1.1 Aim . . . 2

2 Theory **3**
2.1 α-synuclein . . . 3
2.2 Metals in the brain . . . 4
2.2.1 Copper . . . 5
2.2.2 Zinc . . . 6
2.2.3 Iron . . . 6
2.2.4 Manganese . . . 6

3 Methods **9**
3.1 Amyloid formation assay . . . 9
3.2 Circular Dichroism . . . 10
3.3 Atomic Force Microscopy . . . 11
3.4 Transmission Electron Microscopy . . . 11

4 Results **13**
4.1 Fluorescence . . . 13
4.2 Secondary- and tertiary structures . . . 17
4.3 Amyloid fibers . . . 19
4.3.1 AFM . . . 19
4.3.2 TEM . . . 20

5 Discussion and conclusions **23**
5.1 Future work . . . 24

A Appendix **I**

List of Figures

2.1 Left: Micelle-bound α-synuclein monomer, (Ulmer et al., 2005). Right: Structure of part of an α-syn amyloid fibril, (Tuttle et al., 2016). 4
2.2 The three regions of α-syn with annotated common disease-promoting mutations and binding sites for the metal ions Cu(I), Cu(II), Fe(III), Zn(II) and Mn(II). . . 4

3.1 Thioflavin-T chemical structure. 9
3.2 Characteristic CD-spectra for secondary structures; α-helix (green), β-sheet (blue) and unstructured (red). 10

4.1 Comparison of the aggregation curves for the four α-syn variants; wild type, N-terminal acetylated, A53T mutation, and 97 a.a. truncated. 13
4.2 Half-times for the four versions of α-syn, in the presence of the four different metals with increased concentration. 14
4.3 Wild type and N-terminal acetylated α-syn aggregation in the presence of Cu(II) and Fe(III). Top left: WT + Cu(II), top right: acetylated + Cu(II). Bottom left: WT + Fe(III), and bottom right: acetylated + Fe(III). 15
4.4 α-syn A53T in the presence of Cu(II) ions (left), and Fe(III) ions (right). 16
4.5 α-syn variants with notable intensity changes with addition of metals. Top: α-syn WT (left) and A53T (right) in the presence of Mn(II)-ions. Bottom: acetylated α-syn with Fe(III) (left) and Zn(II) (right). 16
4.6 Far-UV CD of α-syn WT with Cu(II) and Zn(II) (left), and acetylated α-syn with Fe(III) and Mn(II) (right). 17
4.7 Near-UV CD of α-syn WT (green), acetylated (blue), and A53T (red) with the addition of Cu(II), as indicated. 18
4.8 α-syn WT (yellow), acetylated (blue) and A53T (red): alone, and with addition of 1:1 metal to the protein ratio. 18
4.9 Top left: α-syn WT amyloid fibrils in AFM. Top right: α-syn WT with 200μM Cu(II)-ions. Bottom left: α-syn WT with an addition of 200μM Fe(III)-ions. Bottom right: α-syn WT with 200μM Mn(II). 19
4.10 Truncated α-syn in the presence of 200μM Cu(II) (left) and 200μM Zn(II) (right). 20
4.11 EM pictures of α-syn A53T in the presence of metals. Left: α-syn A53T alone. Middle: A53T in the presence of 100μM Cu(II). Right: A53T with 100μM Fe(III). 20
4.12 EM pictures of acetylated α-syn in the presence of metals. Left: protein alone. Middle: Acetylated α-syn in the presence of 100μM Cu(II). Right: Acetylated α-syn with 100μM Fe(III). 21

A.1 Aggregation curves for α-syn WT with addition of Zn(II) and Mn(II)-ions. . . . I

A.2 Acetylated α-syn normalized curves for Zn(II) and Mn(II) addition. I
A.3 α-syn A53T normalized curves for Zn(II) and Mn(II) addition. II
A.4 Truncated α-syn aggregation curves for Cu(II), Zn(II), Fe(III), and Mn(II) addition. II
A.5 Example of the gels run to determine if all protein in the samples had aggregated. III

1
Introduction

Our population grows larger in number and increasingly older with the help of modern medicine and better living conditions today, and as a result, age-related diseases have increased substantially in the last 20-25 years (GBD 2016 Parkinson's Disease Collaborators et al., 2018). Neurodegenerative disorders, including Parkinson's disease (PD) and Alzheimer's disease, are the leading cause of death and disability in the world and are among the most studied topics in medicine and pharmaceutics to this date. Despite extensive research, there is still no treatment for these disorders, only medicines that treat the symptoms (Crichton and Ward, 2013a). This in part is because we do not yet understand the mechanisms behind the diseases and that multiple factors are involved in its progression.

PD is a common neurodegenerative age-related disease, that causes both motor system degeneration and cognitive problems. The disease usually affects people around the age of 65, mostly being sporadic in its emergence, however, there are hereditary versions of PD as well (Carboni and Lingor, 2015). The main symptoms of PD are uncontrolled tremors, slowness of speech and movement, and difficulty breathing. The disease is mainly characterized by deterioration of dopamine-producing synapses in substantia nigra pars compacta, located in the ventral midbrain. The affected area is one of the four major dopamine-producing pathways and is largely involved in movement control (Wilshusen and Mosley, 2014). Another hallmark is the abnormal accumulation of cytoplasmic protein aggregates in these neurons. The protein aggregates are called Lewy bodies, and consists of mainly amyloid fibres made out of the protein α-synuclein (α-syn for short) (Spillantini et al., 1998).

In the last five-ten years, the focus has been directed to the involvement of metals in neurological processes, as changes in concentrations and miscompartmentalisation of metal ions have been found in connection with neurodegenerative diseases. Large deposits of iron have been found in Lewy bodies, as well as increased concentration of other divalent metal ions in the brain (Peng et al., 2010). α-syn has been shown to bind metal ions, and such interactions may modulate aggregation. α-syn appears in many forms; sometimes with disease-promoting mutations, and often with post-translational modifications in the form of N-terminal acetylation, phosphorylation or truncation, effectively changing or blocking the metal-binding sites on the protein.

1.1 Aim

This thesis aimed to gain a better understanding of the effects of metal ions on α-syn aggregation into amyloid fibrils. The objective of this thesis was to answer:

How do different metals affect the aggregation kinetics of α-synuclein?

and

Do metal effects depend on α-synuclein variations (e.g. acetylated or truncated etc.)?

Wild type α-syn was compared with an N-terminal acetylated version, a 97 a.a. truncated version to block the C-terminal, as well as the well-known mutation A53T, that has been proven to cause an early-onset form of Parkinson's disease (Crichton and Ward, 2013a). The metals tested are Cu(II), Mn(II), Zn(II) and Fe(III). Here, the focus will be on essential metals, rather than toxic metals that may come from outside the body, as that narrows the scope slightly. Protein purification was not a part of the thesis due to time constraints, and the mutation A53T was chosen due to its proximity to a major copper-binding residue His-50.

2
Theory

This chapter describes the functions and characteristics of α-syn and metals in the brain, and their relationship with one another.

2.1 α-synuclein

α-synuclein is a 140 amino acids long protein, abundantly expressed in presynaptic terminals in the brain, as well as in smaller amounts in other tissues such as muscles and heart. The protein is intrinsically disordered in its native form, and assumes α-helical structure when bound to lipid membranes. New evidence shows that α-syn is N-terminally acetylated in human cells (Moriarty et al., 2014). The normal function of the protein is poorly understood but is thought to be involved in neurotransmitter vesicle transport and maintenance of dopamine (Gentile et al., 2018). Despite the uncertainty of the exact function, α-syn is well studied concerning its aggregation in PD.

One defining neuropathological characteristics of PD is the formation of protein aggregates in the neuronal cytosol (Lewy bodies) containing mostly α-syn amyloid fibers. α-syn can assemble to amyloid fibers; long (in the μm-region), straight, and with an internal structure made up of β-sheets arranged perpendicular to the long axis of the fiber (Krebs et al., 2005). Figure 2.1 left, is showing an α-synuclein monomer bound to a vesicle at the N-terminal, giving the protein α-helical structure. The right picture in figure 2.1 is showing an example of the structure of an amyloid fibril; β-sheets of folded protein layered in a long fiber. There are also occurrences where the protein only forms smaller aggregates of a few monomers, oligomers. It is not currently known if the amyloid fibers or the smaller assemblies, oligomers, are the most toxic in PD.

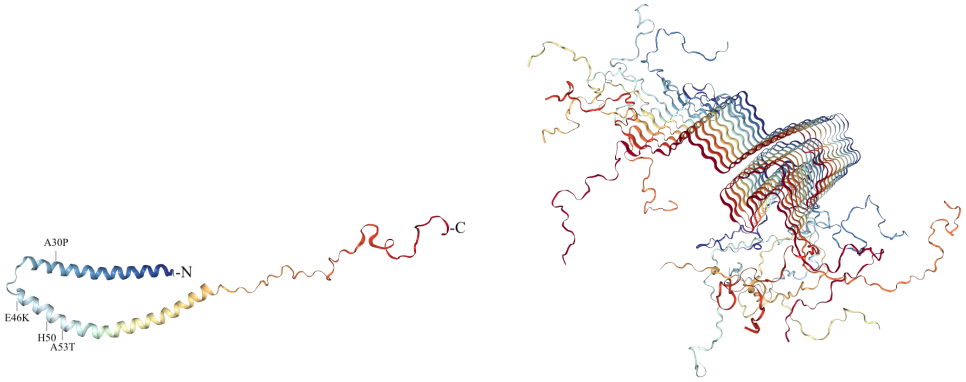

Figure 2.1: Left: Micelle-bound α-synuclein monomer, (Ulmer et al., 2005). Right: Structure of part of an α-syn amyloid fibril, (Tuttle et al., 2016).

There are three regions in the protein; the N-terminal, NAC, and C-terminal, depicted in figure 2.2. The N-terminal (residues 1-60) is involved in lipid interactions, changing secondary structure when bound (figure 2.1, left). NAC (non-amyloid-β component) is the hydrophobic middle region of α-syn (residues 61–95), becomes the core in the amyloid fibrils and adopts a cross β-structure. Finally, the C-terminal (residues 96-140) is a region that appears to temper aggregation (Valiente-Gabioud et al., 2012). Patients with specific mutations of the α-syn gene often show a more aggressive form of PD, with an onset age of PD decreased by about 30 years (Crichton and Ward, 2013a). Some known mutations that are associated with PD are A53T (alanine to threonine), A30P (alanine to proline), E46K (glutamic acid to lysine), as well as others.

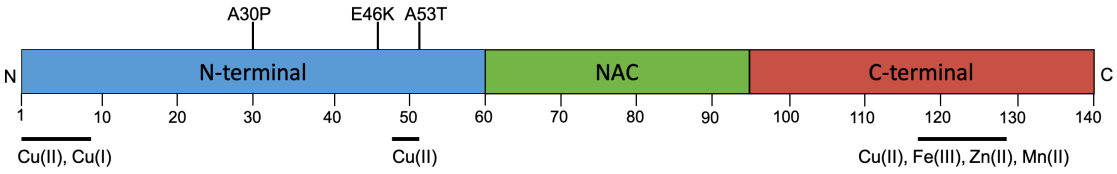

Figure 2.2: The three regions of α-syn with annotated common disease-promoting mutations and binding sites for the metal ions Cu(I), Cu(II), Fe(III), Zn(II) and Mn(II).

2.2 Metals in the brain

Metals are essential in our body to maintain normal function in the body and include iron, lithium, zinc, copper, chromium, nickel, cobalt, vanadium, molybdenum and manganese. These trace metals carry out important functions such as oxygen transport, neurotransmissions, being co-factors in reactions and being involved in the development of the body (Crichton and Ward, 2013b). Some metals are extra important for brain functions and are thus present around and in neurons. Sodium, potassium and calcium is largely responsible for the transmission of neuronal impulses and can be found as free ions being pumped in and out of the cells. Copper,

zinc, and iron are important transition metals that are supplied through the blood-brain barrier to the brain, bound to proteins.

Systemic and tissue imbalances of metal ions are often found in neurodegenerative diseases, thus implying the involvement of metals in the progression or prevention of the disease (McDowall and Brown, 2016; Gaeta and Hider, 2005; Davies et al., 2016). Studies indicate that increase of metals in brain tissue is a consequence of normal aging, and it may be one can be one of the factors promoting age-related neurodegeneration (Valiente-Gabioud et al., 2012). Research indicates that prolonged exposure to iron, copper, zinc or manganese via external factors (e.g. nutrition or industrial work) increases the rate of PD (Valiente-Gabioud et al., 2012).

Even though the direct cause of neurodegeneration in PD is not known, it is possible that oxidative stress can be one reason, due to the increase of redox-active Cu and Fe in the substantia nigra (McDowall and Brown, 2016; Davies et al., 2011). The Fe and Cu- redox cycles result in the production of reactive oxygen species (ROS) that increases oxidative damage in those areas.

Previous *in vitro* research has reported the interaction of metal ions with α-syn, especially copper ions, but also other metals (McDowall and Brown, 2016; Santner and Uversky, 2010). Iron is interesting to investigate, as high concentrations of the metal ion has been found in Lewy bodies of PD patients (Peng et al., 2010). Previous research did not study metal ions systematically and did not have as well prepared α-syn as we do today. Also, α-syn variants have not been compared in parallel for metal binding, and there are conflicting results published (Horvath et al., 2018; Moreau et al., 2018; Atrián-Blasco et al., 2018). Thus, new studies are warranted.

2.2.1 Copper

Copper, both Cu(I) and Cu(II), are important in biochemical processes, including free-radical defense, cellular respiration, neuronal myelination, and iron metabolism (Crichton and Ward, 2013b; Davies et al., 2013). Copper is normally bound to proteins in the cell as Cu(I). However, if there is a lot of ROS present, Cu(I) can be oxidized to Cu(II). Numerous studies have shown Cu to accelerate fibrillisation of α-syn *in vitro*. There is also evidence that Cu(II) increased α-syn aggregation *in vivo*, and increased α-syn concentrations enhanced the sensitivity to copper toxicity (McDowall and Brown, 2016). Copper is known to bind to α-syn in both redox states *in vitro*. Cu(I) are thought to bind at both the N-terminal, coordinating through residues Met-1, Met-5 and forming Cu-O bond at Asp-2, as well as the C-terminal (Met-116 to Met-127). Cu(II) is thought to bind to the same sites, but different ligands than Cu(I), as well as one region extra: His-50 (Binolfi et al., 2010).

As there's new evidence that α-syn is N-terminal acetylated *in vivo*, the high affinity copper binding site is not present *in vivo* (Moriarty et al., 2014). Acetylated α-syn does still have the lower affinity binding sites on NAC and the C-terminal, thus it may retain its copper binding ability.

2.2.2 Zinc

Zinc is a trace metal present in most tissues in the body and plays an important role in brain function and development. In the brain, zinc is mostly bound to zinc metalloproteins inside glial and neuronal cells and act as catalytic and structural co-factors for enzymes. Zn also plays an important role during fetal and early post-natal stage for humans, regulating the development of the brain (Crichton and Ward, 2013b). Deficiency in early life can affect the autonomic nervous system, cerebellar and hippocampal development, thereby leading to e.g. learning impairment. A small percentage of Zn in the brain, is more loosely bound and resides in synaptic vesicles and released during neurotransmission. This extracellular Zn can interact with neuronal transporters, and inhibits N-methyl-D-aspartate receptors (NMDA; glutamate receptor and ion channel protein in neurons); proving to be an important neural messenger both in health and disease (Crichton and Ward, 2013b). Zinc has been shown to speed up the aggregation of α-syn in previous *in vitro*-studies, and there have been reports that Zn(II) is linked to the pathogenesis of PD (Valiente-Gabioud et al., 2012). Studies have also shown that Zn increases in the substantia nigra in patients with PD (Ward, 2015). Valiente-Gabioud et al. found evidence that Zn(II) binds primarily to Asp-121 on the C-terminus, but also Asn-122 and Glu-123, and at higher concentrations ($\geq$300μM) to His-50.

2.2.3 Iron

Iron is the most abundant transition metal and has many roles in the central nervous system (CNS). In the CNS, Fe is used as a cofactor (in heme) in oxygen-transfer in hemoglobin, aids in electron transfer, and takes part in the myelination of axons (Crichton and Ward, 2013b; Davies et al., 2013). Iron is also used as a co-factor in enzymes requiring a redox counter ion; for example hydrogenase, cytochromes or catalase. The concentration Fe varies greatly between regions in the brain, with higher concentrations in areas related to motor function. This localization is due to the fact that Fe has a specific role in dopaminergic neurotransmitter synthesis, involved in movement control (Wilshusen and Mosley, 2014). This could explain the motoric problems in PD, as it is usually associated with higher levels of iron (Crichton and Ward, 2013b). Iron occurs in both oxidation states in the cell, though mainly as Fe(II) due to the hydrolysis of Fe(III) to Fe(II) that occurs in physiological pH of 7.4 (Wilshusen and Mosley, 2014). PD is also characterized by a shift in this Fe(II)/Fe(III) redox-ratio towards Fe(III), as well as an increase of the iron-binding protein ferritin (Santner and Uversky, 2010).

2.2.4 Manganese

Manganese plays an essential role in the metabolism of lipids, carbohydrates, proteins, etc., and is used by many enzymes such as superoxide dismutase and oxalate oxidase (Andreini et al., 2008). There are many instances where manganese over-exposure has led to toxic effects on the body, e.g. mining, welding, or other occupational exposure, where the patients developed PD-like symptoms ("parkinsonism" or "manganism") (Uversky et al., 2001). The overexposure is suggested to

increase oxidative stress inside cells, as well as affecting nuclear pathways such as increased α-syn expression and apoptosis (Carboni and Lingor, 2015). It has thus been speculations that, even though PD and Mn-induced toxicity is different, they might co-operate to trigger neuronal death (Santner and Uversky, 2010). It has been shown that Fe and Mn have a synergistic interaction during the transfer from plasma to the brain in studies with rats (Crichton and Ward, 2013a). This Mn-exposure in the rats led to an increased influx of iron across the blood-brain barrier from the systemic blood circulation, increasing the risk of brain tissue damage. The interaction is mainly between DMT1 (divalent metal transporter 1) transporting Mn(II) to the CNS, and Fpn1 (ferroportin 1; cytoplasmic Fe transporter) being responsible for its efflux (Roth et al., 2013).
Mn(II) can be oxidized to Mn(III), a strong oxidizing agent, in the presence of superoxide (Paris and Segura-Aguilar, 2012). Mn(III) is a part of a degradation chain of dopamine to dopamine o-quinone, a precursor to aminochrome. It can also oxidize thiol groups of proteins and hydroxyl-groups of amino acids thus inactivating enzymes in neurons.

3

Methods

The protein variants used for the project were wild type α-syn, N-terminal acetylated α-syn, 97a.a. truncated α-syn, and α-syn with the A53T mutation. The purified protein, made in the lab by R. Kumar, were stored in a freezer at -80°C until use; then thawed and concentrated (Horvath et al., 2018). The buffer used in the experiments was a Tris-HCl buffer; 0.05M Tris and 0.15M sodium chloride with pH 7.6 at room temperature. The metal ions were Cu(II), Fe(III), Mn(II) and Zn(II). Metal stocks all had a concentration of 2mM, and were made using the salts $CuCl_2$, $FeCl_3$, $MnCl_2$, and $ZnCl_2$ solved in MQ water. The protein sample was run through a gel filtration column (ENrich SEC 70 10 x300, 24ml) before each experiment; making sure that the protein used for each experiment only contained monomers.

3.1 Amyloid formation assay

Amyloid formation kinetics was probed using a fluorescent assay. The assay was conducted using a 96-well plate reader (BMG Labtech, Fluostar Optima) at 37°C, together with 2mm glass beads and the amyloid detecting dye Thioflavin T (ThT), see figure 3.1. The dye binds specifically to amyloid fibrils; bound into the special cross-β structures that make up the amyloids. ThT is non-fluorescent when free in solution, and highly fluorescent when bound to the fibrils (Biancalana and Koide, 2010). This change in fluorescence is due to the structure of the molecule; in solution, it has a dynamic form thus has room to get free of the excitation energy through movement and heat radiation. When ThT is bound to fibrils, however, it is fixed and cannot rotate; the only way to get rid of the excitation energy is emitting light. Excitation wavelength were 440nm, and emission at 490nm. The total run time were 300h, with shaking at 200rpm before each 1200s cycle. The experiment had four replicas per combination of protein and metal, with two repeats. Half-time of the aggregation curves were obtained using a Boltzmann non-linear fit on the normalized aggregation curves.

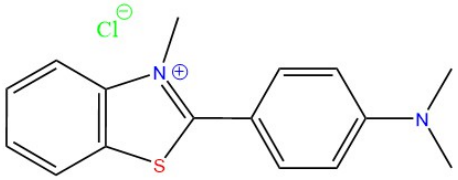

Figure 3.1: Thioflavin-T chemical structure.

3.2 Circular Dichroism

Circular dichroism (CD) was used to detect possible changes in secondary structure of α-syn upon metal additions. CD uses left- and right circularly polarized light to probe chiral molecules. Different secondary structures give rise to their own characteristic CD-spectra in the far-UV region (190-260nm) (Cantor and Schimmel, 1980). An example of a characteristic spectra for α-helix, β-sheet and random coil secondary structure can be seen in Figure 3.2. To be able to compare different measurements, the data had to be normalized to mean residue ellipticity (θ_{MRE}), molar ellipticity independent of peptide length, see equation 3.1.

$$\theta_{MRE} = \frac{\theta_{obs}}{10 \times c \times N \times l} \tag{3.1}$$

θ_{obs} is the obtained signal in mdeg, c the concentration of protein, N the number of peptide bonds of the protein, and l is the cuvette length in cm.

Far-UV CD was collected using both a Jasco J-810 and a Chirascan-CS spectrophotometer, in the region of 190-260nm using a 0.1cm cuvette, with five repeats per run. The protein was also investigated in near-UV region of 250-440nm using a 1cm glass cuvette, with three repeats per run. In the near-UV region, tertiary structure and metal-interactions may be detectable.

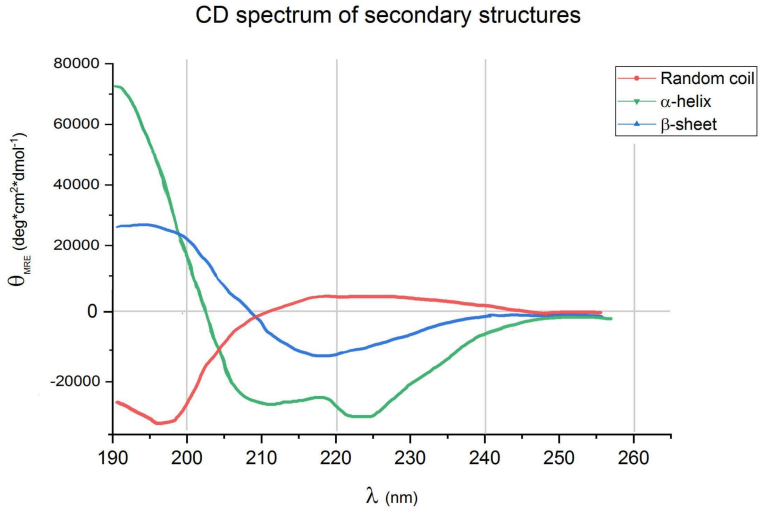

Figure 3.2: Characteristic CD-spectra for secondary structures; α-helix (green), β-sheet (blue) and unstructured (red).

3.3 Atomic Force Microscopy

Atomic force microscopy (AFM) was conducted on some α-syn aggregation samples. A surface of mica was used for all experiments. AFM is a molecular imaging method, used to determine size and shape of molecules and complexes on a flat surface. The method is a good complement to the aggregation assays; we can see if the protein actually aggregated, and if they form amyloids or amorphous aggregates. Aggregated samples were deposited onto newly cleaved mica after being diluted with MilliQ water 10 times. After 10 minutes, the excess was dried off with filter paper and the mica washed two times with MilliQ water before being dried with a stream of nitrogen gas. The images were obtained using a gold-coated single crystal silicon cantilever (NT-MDT, NSG01, 5.1N/m spring constant) on a NTREGA Prima set-up, at a resonance frequency of around 180 kHz (Horvath et al., 2018). The images were obtained with a 0.5Hz scan rate and were analysed with WSxM 5.0, a software for scanning probe microscopy (Horcas et al., 2007).

3.4 Transmission Electron Microscopy

Electron microscopy (TEM) was performed as a complement to AFM, as the AFM was not always working. TEM is another imaging method that uses a beam of electrons as illumination. The electrons scatter as the beam travels through the sample, and thus creates a 2D image containing structural information about the sample (Pielach and Micaroni, 2018). The microscope used in this project was a TALOS L120C, using high contrast imaging with a spot size of 2 or 3, and magnification mode set around SA 17500x-300000x. The sample was negatively stained with 1% phosphtungstate (PTA) solved in MQ-water, after grids had been glow discharged to be more hydrophilic. The camera used for high resolution image acquisition was a Ceta 4x4 K camera, with 1s integration time, binning 1, and 4 frames per exposure time.

4

Results

The results from all experiments performed in this thesis are presented below. This includes graphs from the kinetic assays, CD-spectra and analyses of the formed aggregation species by AFM and TEM.

4.1 Fluorescence

The aggregation assays had one repetition and with four replicas each time. Most of the results from the aggregation assays can be found in Appendix 1, due to the magnitude of combinations that emerge from four protein variations coupled with four different metals. The aggregation of the four versions of α-syn is presented in figure 4.1, showing the already prominent difference in aggregation kinetics without addition of metal ions. Truncated α-syn and the mutation A53T give very similar curves, being the fastest to aggregate out of the four. Acetylated α-syn is faster than the non-acetylated, but not to the extent of the mutated and truncated.

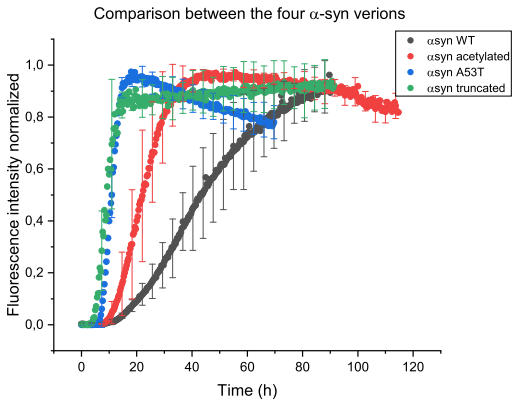

Figure 4.1: Comparison of the aggregation curves for the four α-syn variants; wild type, N-terminal acetylated, A53T mutation, and 97 a.a. truncated.

Figure 4.2 is visualizing the shift in half-time when metals are added to α-synuclein during aggregation. Half-time is the time to reach halfway to stationary phase, when all protein has aggregated. As one can see in figure 4.2 top left, the half time for α-syn WT aggregation is affected by all the tested metals except Mn(II). Both Cu(II) and Fe(III) decreased the half-time to 50% with the addition of 1 equivalent of metal to protein. Zinc's effect on aggregation is less stable and oscillates up and down with concentration, something that has been observed in several replications.

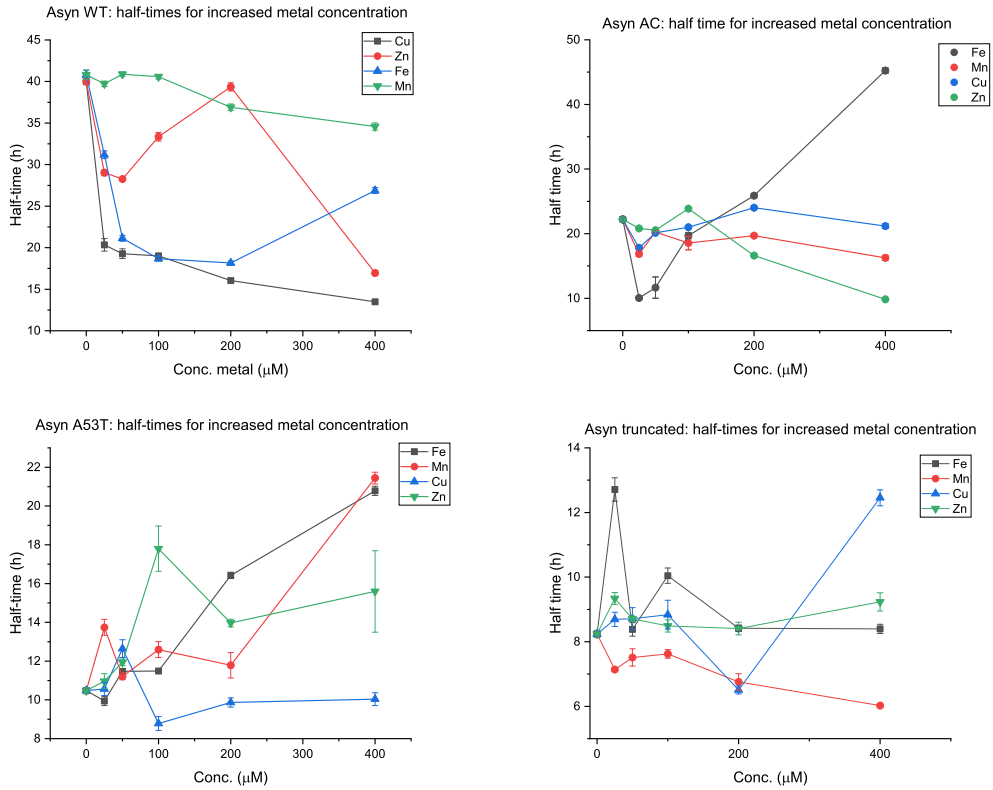

Figure 4.2: Half-times for the four versions of α-syn, in the presence of the four different metals with increased concentration.

N-terminal acetylated α-syn aggregation is less affected by the addition of metal ions (figure 4.2, top right). Fe(III) addition does increase the half-time at lower concentrations (25-100μM) and decrease it at concentrations above 200μM (1:4 protein:metal ratio). The same can be observed in figure 4.3 showing the aggregation curves for wild type and acetylated α-syn in the presence of copper and iron. Here, one can see that there are two types of changes when adding metals; effects on primary nucleation and secondary nucleation/elongation. Primary nucleation is the shift of lag-phase in time, depending on the concentration monomer in the solution (Meisl et al., 2016). An effect on primary nucleation is apparent for acetylated α-syn with added Fe(III). Secondary nucleation depends on both aggregate mass and monomers. Effects on secondary nucleation can be observed for acetylated α-syn in the presence of higher concentrations Fe(III) (figure 4.3, bottom left). α-syn WT with Cu(II) seems to exhibit a mix of both primary and secondary nucleation, shifting both lag-phase and slope.

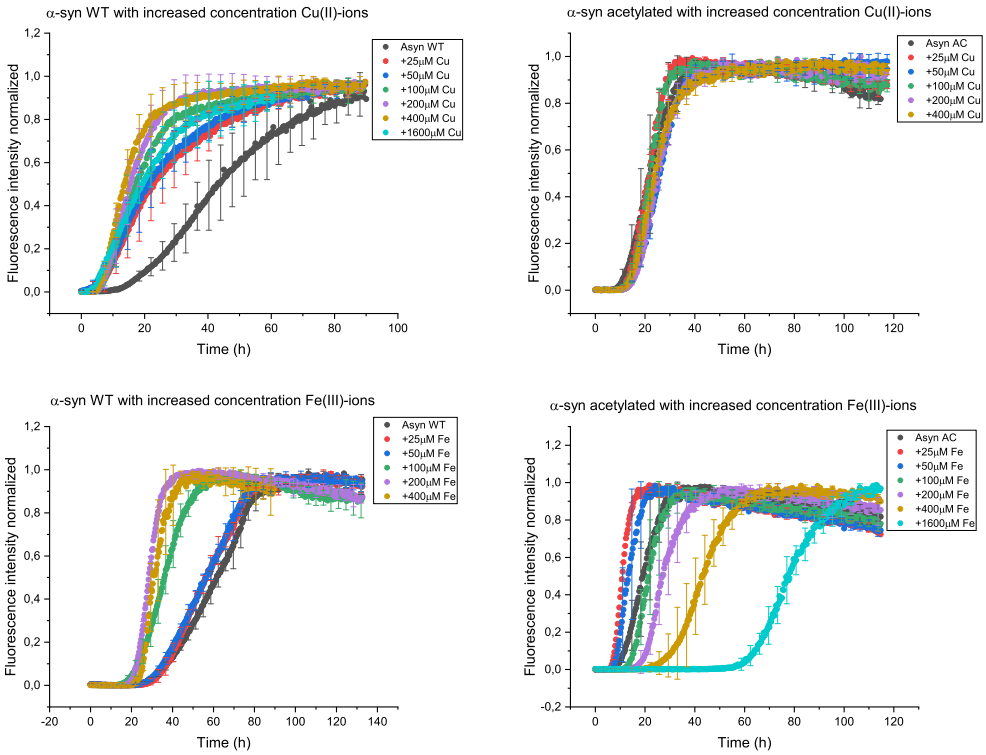

Figure 4.3: Wild type and N-terminal acetylated α-syn aggregation in the presence of Cu(II) and Fe(III). Top left: WT + Cu(II), top right: acetylated + Cu(II). Bottom left: WT + Fe(III), and bottom right: acetylated + Fe(III).

The addition of Cu(II) to A53T α-syn gave no change in aggregation, see figure 4.4 left. Fe(III) ions only affected the mutated protein at concentrations above 200μM, slowing down aggregation like acetylated α-syn in presence of higher concentrations of Fe(III) (figure 4.4, right).

Manganese ions were also tested for all four α-syn variants, but did not affect aggregation kinetics when inspecting the normalized curves (see Appendix A, figures A.1 to A.4). However, Mn(II) seemed to have an effect on the ThT intensity of α-syn WT and A53T, lowering the final intensity for both (figure 4.5). The lower intensity suggest that less amyloid fibers are formed in the aggregation process, or emission is quenched by Mn(II). Figure 4.5 is showing aggregation curves without normalization, giving an indication of the relative amount amyloids formed. Fe(III) and Zn(II) seems to affect acetylated α-syn by reducing intensity relative to the protein alone. For Fe(III) this is only after 100μM addition to the protein however. Truncated α-syn was not affected by the addition of any of the four metal ions (Appendix A figure A.4).

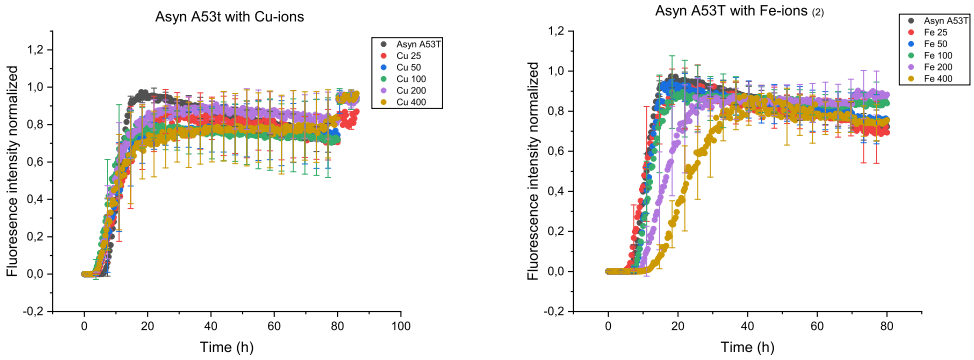

Figure 4.4: α-syn A53T in the presence of Cu(II) ions (left), and Fe(III) ions (right).

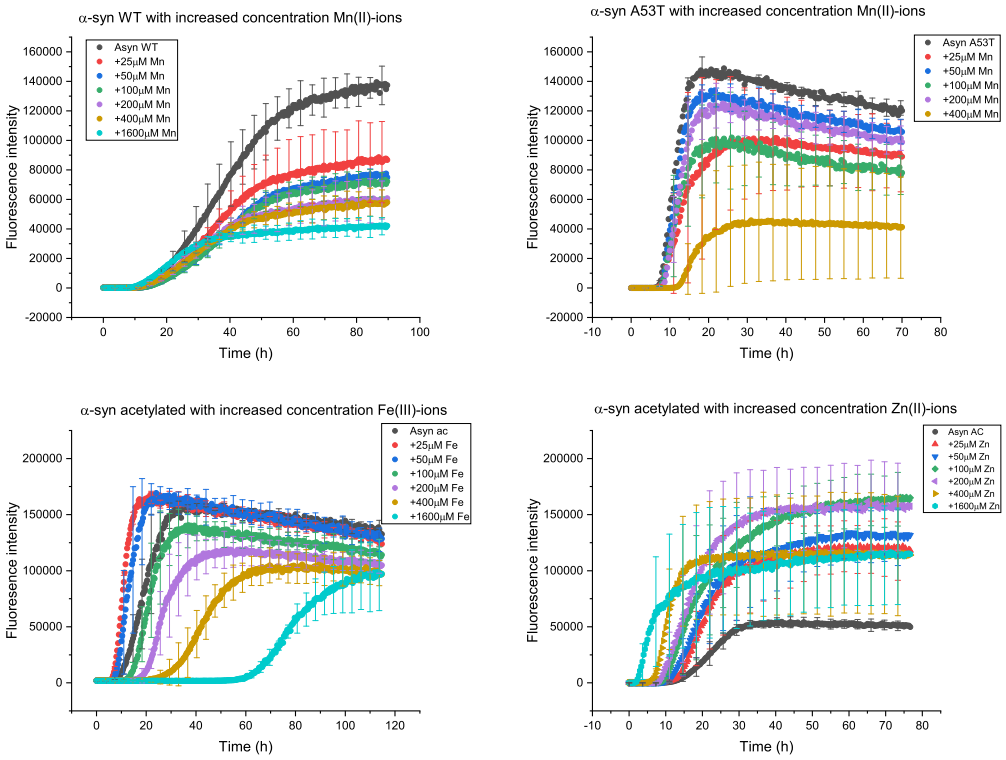

Figure 4.5: α-syn variants with notable intensity changes with addition of metals. Top: α-syn WT (left) and A53T (right) in the presence of Mn(II)-ions. Bottom: acetylated α-syn with Fe(III) (left) and Zn(II) (right).

Table 4.1: The results from the different protein variant and metal combinations. Increase in aggregation is represented by a plus (+), decrease in aggregation a minus (-), and no change a zero (0).

	α-syn WT	**α-syn acetylated**	**α-syn truncated**	**α-syn A53T**
Cu(II)	+	**0**	**0**	**0**
Fe(III)	+	-	**0**	**- (≥ 400)**
Zn(II)	**0**	**+ (≥ 200μM)**	**0**	**0**
Mn(II)	**0**	**0**	**0**	**0**

4.2 Secondary- and tertiary structures

I used CD in far-UV and near-UV regions to assess interactions between metal and protein.

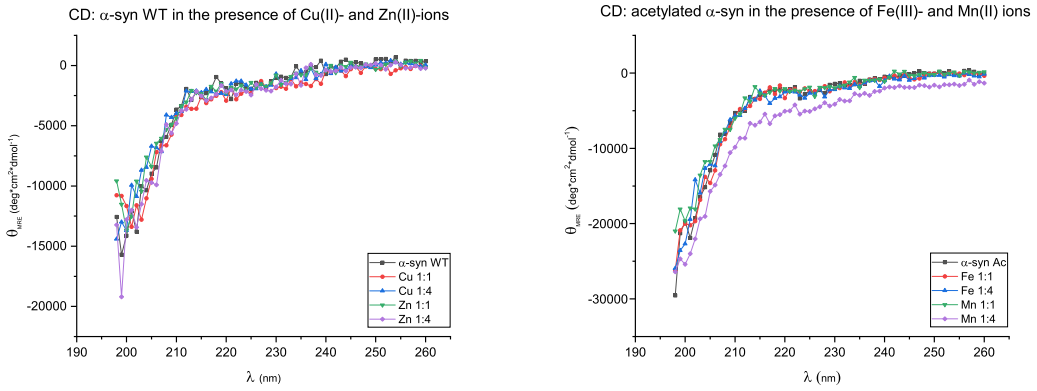

Figure 4.6: Far-UV CD of α-syn WT with Cu(II) and Zn(II) (left), and acetylated α-syn with Fe(III) and Mn(II) (right).

Figure 4.6 depicts the far-UV CD spectra from α-syn WT and acetylated. No changes in the CD spectra could be seen when metals were added, showing that α-syn is unstructured in solution and does not gain structure when metals bind. Truncated was not tested due to it being essentially a shorter version of the wild type.

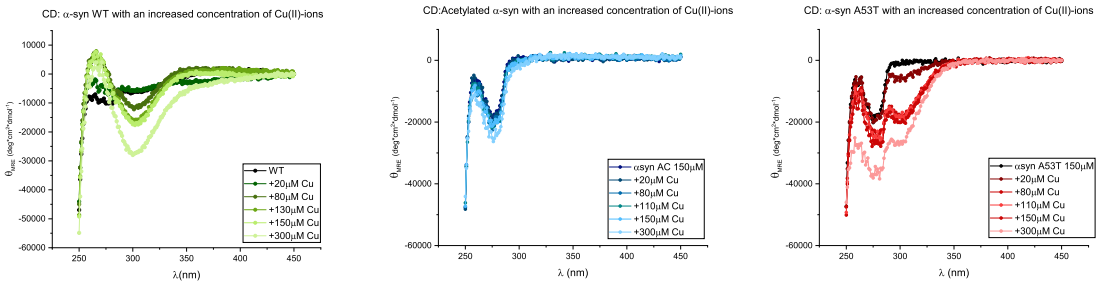

Figure 4.7: Near-UV CD of α-syn WT (green), acetylated (blue), and A53T (red) with the addition of Cu(II), as indicated.

Figure 4.7 shows near-UV CD for α-syn WT, acetylated, and A53T with addition of Cu(II)-ions in different concentrations, to probe for metal-interaction. There is a clear difference between the α-syn variants suggesting different binding of copper. α-syn WT has a clear negative peak at 300nm, becoming more negative with increased Cu(II)-concentration. This can be a ligand to metal charged transfer absorption at 300nm, consistent with results from previous research (Binolfi et al., 2010). Binolfi et al. suggests the interaction to be between a deprotonated peptide amide at Asp-2, Met-1 and the copper ion. α-syn A53T exhibited similar changes in CD-spectra as the wild type (see figure 4.7, right). A53T has a negative peak at 300nm, but the signal is slightly different, with an additional negative peak at 275nm, suggesting an altered Cu(II)-binding site, possibly at His-50 and Thr-53. Figure 4.8 compares the three protein variants; at a ratio of 1:0 and 1:1 protein to metal. Wild type and A53T show similar changes when Cu(II) binds, with a negative peak at 300nm. Acetylated α-syn did not show any changes upon Cu-addition, suggesting that Cu(II) does not bind or at least do not form a CD-active interaction.

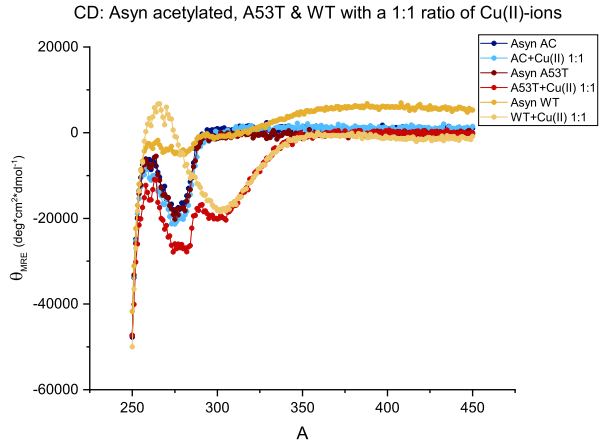

Figure 4.8: α-syn WT (yellow), acetylated (blue) and A53T (red): alone, and with addition of 1:1 metal to the protein ratio.

4.3 Amyloid fibers

To visualize the formed fibers, both AFM and TEM was utilized. The samples for imaging was prepared after ThT fluorescence experiments, but since the AFM had problems in the start of the project, not all samples could be used for imaging. Due to these time and protein constraints, some data is missing here.

4.3.1 AFM

The amyloid fibrils were probed by an AFM. In these samples concentration of metals were 200μM of the metals.

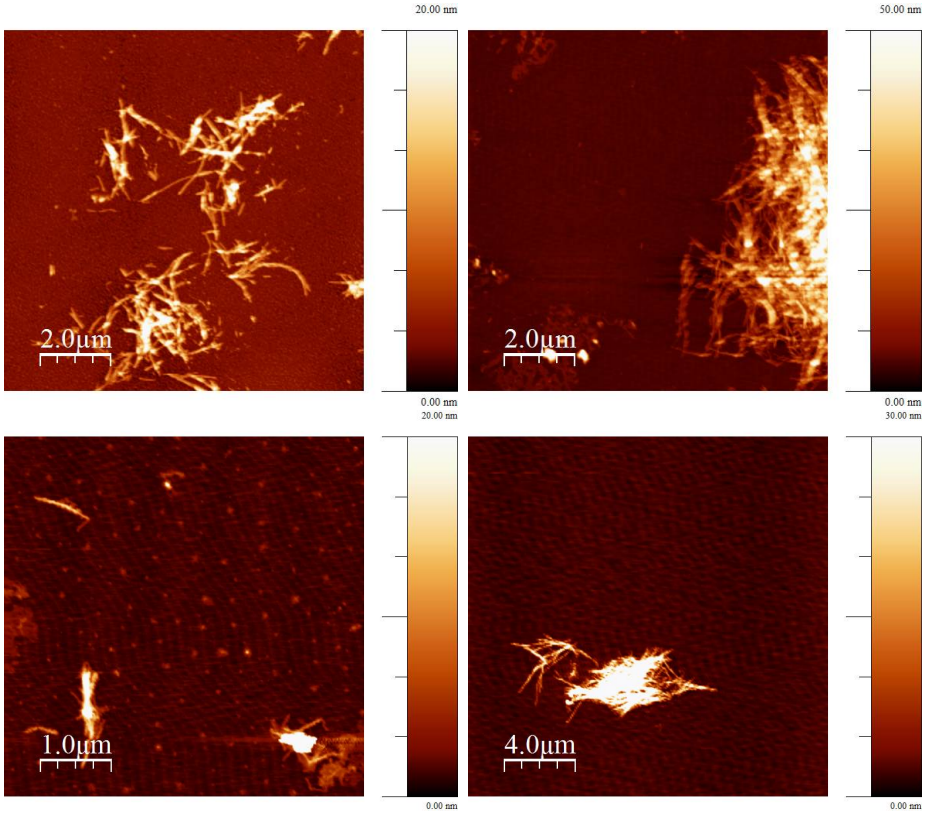

Figure 4.9: Top left: α-syn WT amyloid fibrils in AFM. Top right: α-syn WT with 200μM Cu(II)-ions. Bottom left: α-syn WT with an addition of 200μM Fe(III)-ions. Bottom right: α-syn WT with 200μM Mn(II).

Figure 4.9 shows AFM for α-syn WT; top left is the protein alone, top right with addition of Cu(II), bottom left addition of Fe(III), and bottom right has an addition of Mn(II). α-syn WT had amyloid fibers with heights of 6-8nm. WT + Cu(II) also formed amyloid fibers of similar height, with the addition of some amorphous aggregates in the mix. The sample with Fe(III) still showed a few amyloid fibers, but also contained smaller particles, possibly α-syn oligomers. Mn(II) with α-syn WT resulted in amyloid fiber clusters.

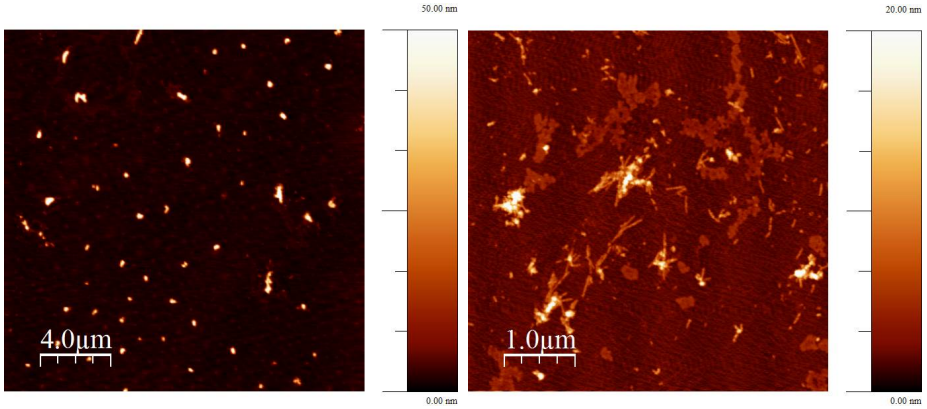

Figure 4.10: Truncated α-syn in the presence of 200μM Cu(II) (left) and 200μM Zn(II) (right).

Figure 4.10 shows AFM of truncated α-syn in the presence of Cu(II) (fig 4.10, left) and Zn(II) (fig 4.10, right). Despite the ThT data, addition of Cu resulted in no amyloid fiber formations, instead there were 50nm dots of aggregated protein, possibly α-syn oligomers. Zn was added to the truncated protein, there were 6-7nm high amyloid fibers as well as amorphous aggregates. The fibers in the truncated samples were shorter and there were more amorphous aggregates than for the wild type samples (figure 4.9).

4.3.2 TEM

Figure 4.11 shows TEM of the aggregates of α-syn A53T, alone and in the presence of Cu(II) and Fe(III). As the pictures show, there was no apparent difference in amyloid fiber formation; they all formed long fibers and no amorphous aggregates. No height measurements could be obtained here.

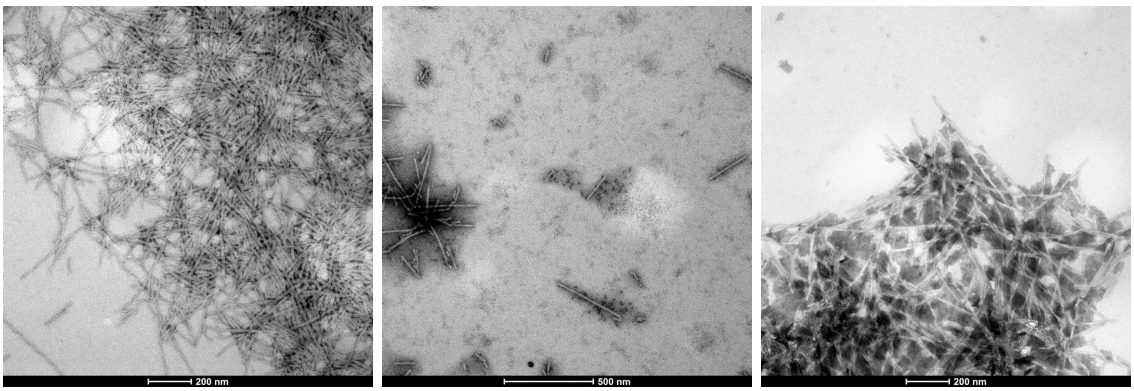

Figure 4.11: EM pictures of α-syn A53T in the presence of metals. Left: α-syn A53T alone. Middle: A53T in the presence of 100μM Cu(II). Right: A53T with 100μM Fe(III).

Figure 4.12 shows aggregates of acetylated α-syn, alone and in the presence of Cu(II) and Fe(III). Acetylated protein displayed amyloid fibrils similar to WT. Cu(II) addition to the acetylated protein mad no difference visually to the fibers. The addition of Fe(III) resulted in large amounts of amyloids, covering the entire field of view.

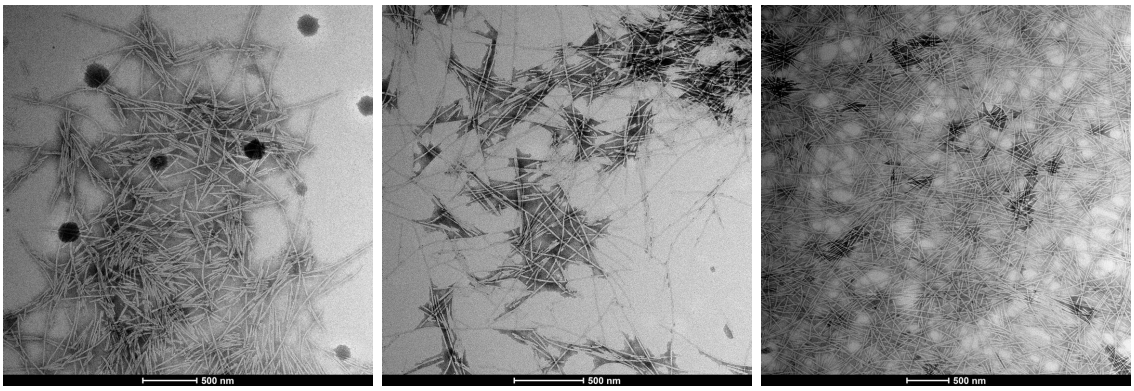

Figure 4.12: EM pictures of acetylated α-syn in the presence of metals. Left: protein alone. Middle: Acetylated α-syn in the presence of 100μM Cu(II). Right: Acetylated α-syn with 100μM Fe(III).

5

Discussion and conclusions

The results in the previous chapter gave good insight how the different metals affected α-syn aggregation kinetics. Both Zn(II) and Mn(II) that were chosen as possible candidates for affecting this; gave next to no response to any version of the protein. The fibrils formed in presence of the metals further confirmed that, indeed amyloids formed, and they maintained the same shape and length as in absence of metals (figures 4.9 and 4.10). Combining these results with previous knowledge of the metals' role in the brain, one can hypothesize that Zn and Mn affect the progression of the disease indirectly.

Addition of Cu(II) to α-syn WT resulted in a significant increase in aggregation rate, which also has been shown in previous studies. Near-UV CD for α-syn WT with Cu(II) showed a negative peak at 300nm; indicative of metal-ligand charge transfer involving a deprotonated peptide amide, previously suggested as Asp2 (Binolfi et al., 2010). Cu(II) was suggested to interact with N-terminus, Asp-2 and Met-1. α-syn A53T also binds Cu(II), (figure 4.8), suggesting an altered Cu-site, perhaps towards His50 and Thr53 instead.

The near-UV CD curves for A53T shifts down at 300nm until a metal concentration of 300μM (2:1 metal to protein ratio). This would mean that α-syn A53T binds 2 equivalents of Cu(II). For α-syn WT, there is no shift beyond 1:1 ratio (150μM in figure 4.7), suggesting a 1:1 Cu(II)-complex formation. However, when WT is normalized for 450nm around zero, the peak at 300nm continues to go down for a Cu(II):protein ratio of 2:1. This suggests that more copper can bind, and indeed Binolfi et.al. has described the same phenomenon for wild type α-syn, where they looked at a longer wavelength spectra from 250 to 800nm (Binolfi et al., 2010). They found a positive peak at 520nm and a negative peak at 650nm corresponding to 2 equivalents of metal bound. This broader wavelength band would be something to look into with further studies.

There was no binding of Cu(II) to acetylated α-syn detected in the Near-UV CD spectra, in accord with the N-terminus being of high importance (Moriarty et al., 2014). In support, aggregation of acetylated α-syn showed little effect by Cu(II) addition (figure 4.2 top right). If copper still is binding, it is to the lower affinity binding site on the C-terminal but does not affect the aggregation of the protein. The only metal that changes the aggregation kinetics of acetylated α-syn was Fe(III). There is an interesting difference in the effect of Fe(III) on α-syn WT versus acetylated α-syn. Fe(III) slows down the aggregation when over 100μM is added for

acetylated, but keeps speeding up the process for WT. As previously mentioned, α-syn is most likely acetylated *in vivo*, indicating that Fe(III) may be protective.

Images obtained showed that in all cases, amyloids were the main formed species of aggregates, with the occasional amorphous aggregates in the mix. Acetylated α-syn in the presence of Fe(III) did form some oligomeric structures as well as amyloids. According to previous studies, at least Fe(II) is known to promote oligomer formation in α-syn (Gentile et al., 2018). Perhaps some Fe(III) got reduced to Fe(II), or the both redox states may have this oligomeric effect on the protein, at different degrees. Truncated α-syn with Cu(II) however, only formed spherical (50nm) oligomers, and no amyloids. This means that the interaction of Cu(II) to the N-terminus, with the absence of a C-terminus, prevents full amyloid formation. Unfortunately, not much data were obtained on the truncated fibers, leaving that to be an interesting subject for future studies.

5.1 Future work

There are a lot left to discover to fully understand the cause and progression of Parkinson's disease and the effect of metals on the reactions. A lot of research has already contributed a good base, but with recent discoveries of acetylation and the involvement of Fe(III)-ions, rather than Fe(II) that has been more extensively studied before.

It is also worth looking into mutants and other versions of α-syn, with acetylation as well. For example the disease causing mutant A53T, that has been studied in this thesis, would be interesting to study in acetylated form together with metals to see if there are differences from the results obtained here. As all forms of α-syn might be acetylated *in vivo*, that should be the main focus in the future. It would be interesting to utilize NMR to determine where the metal binds to the acetylated protein variants and compare to previous research.

Further work into visualizing the amyloid fibers should be a goal for future studies, as not all could be done in this thesis. As Zn(II) and Mn(II) did not affect the speed of the reactions, maybe they invoke other changes to the amyloids. To study these metals together may also give deeper insights to the pathological interactions resulting in PD.

References

Andreini, C., Bertini, I., Cavallaro, G., Holliday, G. L. and Thornton, J. M. (2008). Metal ions in biological catalysis: from enzyme databases to general principles. JBIC Journal of Biological Inorganic Chemistry *13*, 1205–1218.

Atrián-Blasco, E., Gonzalez, P., Santoro, A., Alies, B., Faller, P. and Hureau, C. (2018). Cu and Zn coordination to amyloid peptides: From fascinating chemistry to debated pathological relevance. Coordination Chemistry Reviews *371*, 38–55.

Biancalana, M. and Koide, S. (2010). Molecular mechanism of Thioflavin-T binding to amyloid fibrils. Biochimica et Biophysica Acta (BBA) - Proteins and Proteomics *1804*, 1405–1412.

Binolfi, A., Rodriguez, E. E., Valensin, D., D'Amelio, N., Ippoliti, E., Obal, G., Duran, R., Magistrato, A., Pritsch, O., Zweckstetter, M., Valensin, G., Carloni, P., Quintanar, L., Griesinger, C. and Fernandez, C. O. (2010). Bioinorganic Chemistry of Parkinson's Disease: Structural Determinants for the Copper-Mediated Amyloid Formation of Alpha-Synuclein. Inorganic Chemistry *49*, 10668–10679.

Cantor, C. and Schimmel, P. (1980). Part II. Techniques for the study of biological structure and function. In Biophysical chemistry pp. 409–433. W.H. Freeman.

Carboni, E. and Lingor, P. (2015). Insights on the interaction of alpha-synuclein and metals in the pathophysiology of Parkinson's disease. Metallomics *7*, 395–404.

Crichton, R. and Ward, R. (2013a). Parkinson's Disease. In Metal-Based Neurodegeneration chapter 6, pp. 131–145. John Wiley & Sons, Incorporated Chichester, United Kingdom 2 edition.

Crichton, R. and Ward, R. (2013b). Role of Metal Ions in Brain Function, Metal Transport, Storage and Homoeostasis. In Metal-based Neurodegeneration chapter 2, pp. 23–50. John Wiley and Sons Ltd Chichester, United Kingdom 2 edition.

Davies, K. M., Hare, D. J., Cottam, V., Chen, N., Hilgers, L., Halliday, G., Mercer, J. F. B. and Double, K. L. (2013). Localization of copper and copper transporters in the human brain. Metallomics : integrated biometal science *5*, 43–51.

Davies, K. M., Mercer, J. F. B., Chen, N. and Double, K. L. (2016). Copper dyshomoeostasis in Parkinson's disease: implications for pathogenesis and indications for novel therapeutics. Clinical Science *130*, 565–574.

Davies, P., Moualla, D. and Brown, D. R. (2011). Alpha-Synuclein Is a Cellular Ferrireductase. PLoS ONE *6*, e15814.

Gaeta, A. and Hider, R. C. (2005). The crucial role of metal ions in neurodegeneration: the basis for a promising therapeutic strategy. British journal of pharmacology *146*, 1041–59.

GBD 2016 Parkinson's Disease Collaborators, E. R., Elbaz, A., Nichols, E., Abd-Allah, F., Abdelalim, A., Adsuar, J. C., Ansha, M. G., Brayne, C., Choi, J.-Y. J., Collado-Mateo, D., Dahodwala, N., Do, H. P., Edessa, D., Endres, M., Fereshtehnejad, S.-M., Foreman, K. J., Gankpe, F. G., Gupta, R., Hankey, G. J., Hay, S. I., Hegazy, M. I., Hibstu, D. T., Kasaeian, A., Khader, Y., Khalil, I., Khang, Y.-H., Kim, Y. J., Kokubo, Y., Logroscino, G., Massano, J., Ibrahim, N. M., Mohammed, M. A., Mohammadi, A., Moradi-Lakeh, M., Naghavi, M., Nguyen, B. T., Nirayo, Y. L., Ogbo, F. A., Owolabi, M. O., Pereira, D. M., Postma, M. J., Qorbani, M., Rahman, M. A., Roba, K. T., Safari, H., Safiri, S., Satpathy, M., Sawhney, M., Shafieesabet, A., Shiferaw, M. S., Smith, M., Szoeke, C. E. I., Tabarés-Seisdedos, R., Truong, N. T., Ukwaja, K. N., Venketasubramanian, N., Villafaina, S., weldegwergs, K. g., Westerman, R., Wijeratne, T., Winkler, A. S., Xuan, B. T., Yonemoto, N., Feigin, V. L., Vos, T. and Murray, C. J. L. (2018). Global, regional, and national burden of Parkinson's disease, 1990-2016: a systematic analysis for the Global Burden of Disease Study 2016. The Lancet. Neurology *17*, 939–953.

Gentile, I., Garro, H. A., Delgado Ocaña, S., Gonzalez, N., Strohäker, T., Schibich, D., Quintanar, L., Sambrotta, L., Zweckstetter, M., Griesinger, C., Menacho Márquez, M. and Fernández, C. O. (2018). Interaction of Cu(i) with the Met-X ₃ -Met motif of alpha-synuclein: binding ligands, affinity and structural features. Metallomics *10*, 1383–1389.

Horcas, I., Fernández, R., Gómez-Rodríguez, J. M., Colchero, J., Gómez-Herrero, J. and Baro, A. M. (2007). WSXM : A software for scanning probe microscopy and a tool for nanotechnology. Review of Scientific Instruments *78*, 013705.

Horvath, I., Werner, T., Kumar, R. and Wittung-Stafshede, P. (2018). Copper chaperone blocks amyloid formation via ternary complex. Quarterly Reviews of Biophysics *51*, e6.

Krebs, M., Bromley, E. and Donald, A. (2005). The binding of thioflavin-T to amyloid fibrils: localisation and implications. Journal of Structural Biology *149*, 30–37.

McDowall, J. S. and Brown, D. R. (2016). Alpha-synuclein: relating metals to structure, function and inhibition. Metallomics : integrated biometal science *8*, 385–97.

Meisl, G., Kirkegaard, J. B., Arosio, P., Michaels, T. C. T., Vendruscolo, M., Dobson, C. M., Linse, S. and Knowles, T. P. J. (2016). Molecular mechanisms of protein aggregation from global fitting of kinetic models. Nature Protocols *11*, 252–272.

Moreau, C., Duce, J. A., Rascol, O., Devedjian, J.-C., Berg, D., Dexter, D., Ca-

bantchik, Z. I., Bush, A. I. and Devos, D. (2018). Iron as a therapeutic target for Parkinson's disease. Movement Disorders *33*, 568–574.

Moriarty, G. M., Minetti, C. A. S. A., Remeta, D. P. and Baum, J. (2014). A Revised Picture of the Cu(II) α-Synuclein Complex: The Role of N-Terminal Acetylation. Biochemistry *53*, 2815–2817.

Paris, I. and Segura-Aguilar, J. (2012). The role of metal ions in dopaminergic neuron degeneration in Parkinsonism and Parkinson's disease. In Metal Ions in Neurological Systems pp. 31–39. Springer Vienna Vienna.

Peng, Y., Wang, C., Xu, H. H., Liu, Y.-N. and Zhou, F. (2010). Binding of α-synuclein with Fe(III) and with Fe(II) and biological implications of the resultant complexes. Journal of Inorganic Biochemistry *104*, 365–370.

Pielach, A. and Micaroni, M. (2018). TEM - TALOS L120C User manual. Technical report Centre for Cellular Imaging, Core Facilities, the Sahlgrenska Academy. Univ. of Gothenburg Gothenburg.

Roth, J., Ponzoni, S. and Aschner, M. (2013). Manganese Homeostasis and Transport. pp. 169–201. Springer, Dordrecht.

Santner, A. and Uversky, V. N. (2010). Metalloproteomics and metal toxicology of α-synuclein. Metallomics *2*, 378.

Spillantini, M. G., Crowther, R. A., Jakes, R., Hasegawa, M. and Goedert, M. (1998). alpha-Synuclein in filamentous inclusions of Lewy bodies from Parkinson's disease and dementia with lewy bodies. Proceedings of the National Academy of Sciences of the United States of America *95*, 6469–73.

Tuttle, M., Comellas, G., Nieuwkoop, A., Covell, D., Berthold, D., Kloepper, K., Courtney, J., Kim, J., Barclay, A., Kendall, A., Wan, W., Stubbs, G., Schwieters, C., Lee, V., George, J. and Rienstra, C. (2016). Solid-state NMR structure of a pathogenic fibril of full-length human alpha-synuclein. Nat.Struct.Mol.Biol. *23*, 409–415.

Ulmer, T., Bax, A., Cole, N. and Nussbaum, R. (2005). Structure and dynamics of micelle-bound human alpha-synuclein. J.Biol.Chem. *280*, 9595–9603.

Uversky, V. N., Li, J. and Fink, A. L. (2001). Metal-triggered structural transformations, aggregation, and fibrillation of human alpha-synuclein. A possible molecular NK between Parkinson's disease and heavy metal exposure. The Journal of biological chemistry *276*, 44284–96.

Valiente-Gabioud, A. A., Torres-Monserrat, V., Molina-Rubino, L., Binolfi, A., Griesinger, C. and Fernández, C. O. (2012). Structural basis behind the interaction of Zn2+ with the protein α-synuclein and the Aβ peptide: A comparative analysis. Journal of Inorganic Biochemistry *117*, 334–341.

Ward, R. J. (2015). Ageing neuroinflammation and neurodegeneration. Frontiers in Bioscience *7*, 433.

Wilshusen, R. A. and Mosley, R. L. (2014). Innate and Adaptive Immune-Mediated Neuroinflammation and Neurodegeneration in Parkinson's Disease. In Neuroinflammation and Neurodegeneration pp. 119–142. Springer New York New York, NY.

A

Appendix

Aggregation curves for the ThT-spectroscopy assays conducted during the thesis.

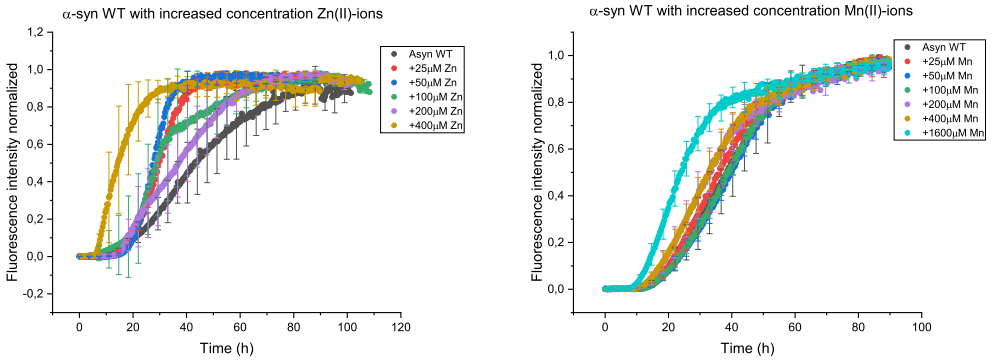

Figure A.1: Aggregation curves for α-syn WT with addition of Zn(II) and Mn(II)-ions.

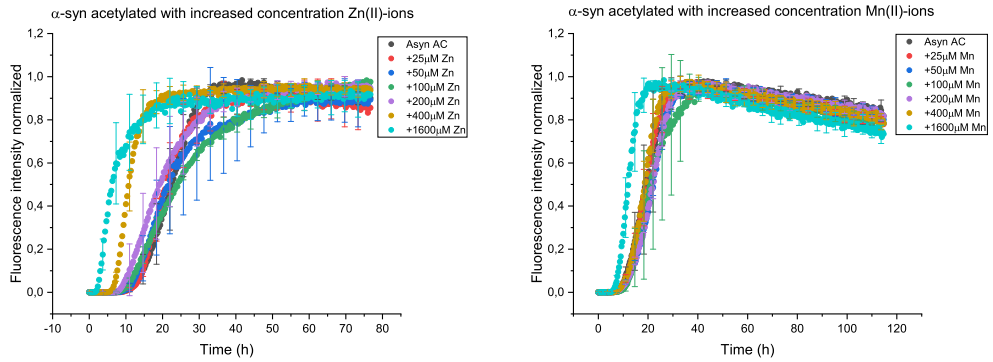

Figure A.2: Acetylated α-syn normalized curves for Zn(II) and Mn(II) addition.

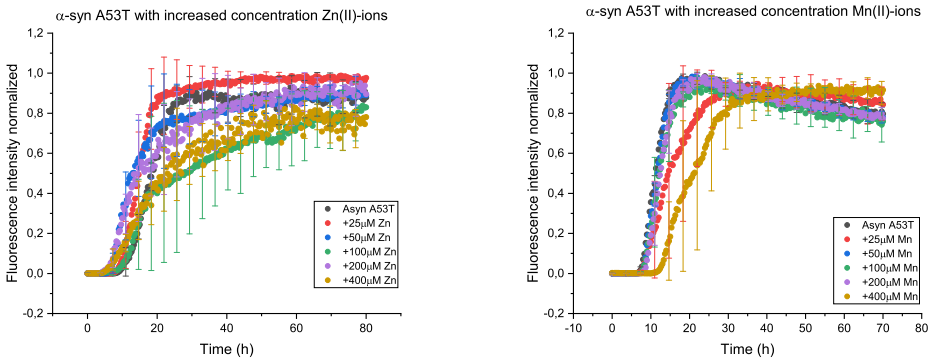

Figure A.3: α-syn A53T normalized curves for Zn(II) and Mn(II) addition.

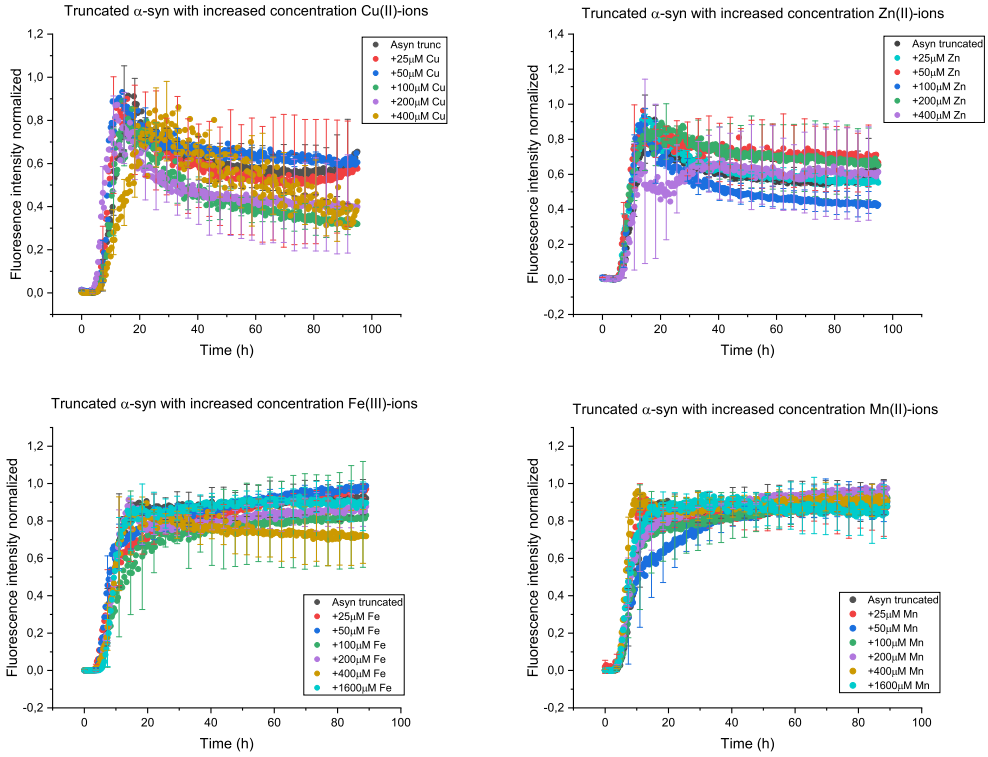

Figure A.4: Truncated α-syn aggregation curves for Cu(II), Zn(II), Fe(III), and Mn(II) addition.

Figure A.5 is showing an example of how the gels looked when testing if the ThT-fluorescence samples had aggregated fully. To the far left is a protein ladder, well 2 holds the sample before aggregation (t=0h), and the seven following wells contain the different protein-metal combinations after it had been allowed to fully aggregate (ca. 100h). As one can see, the wells are all empty except for t=0, indicating that there is no monomers left in the samples after 100h - everything had aggregated.

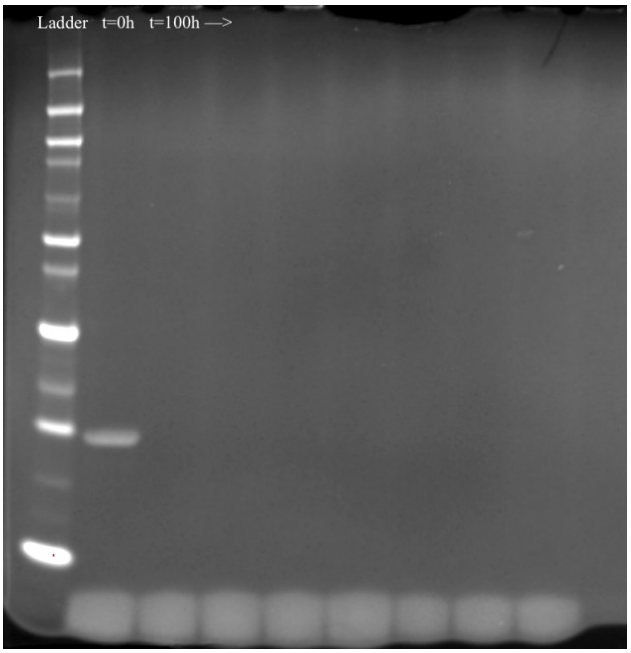

Figure A.5: Example of the gels run to determine if all protein in the samples had aggregated.